Role of Electrophilic and General Base Catalysis in the Mechanism of *Escherichia coli* Uracil DNA Glycosylase†

Alexander C. Drohat, Jayashree Jagadeesh, Eric Ferguson, and James T. Stivers*

Center for Advanced Research in Biotechnology of the University of Maryland Biotechnology Institute and the National Institute for Standards and Technology, 9600 Gudelsky Drive, Rockville, Maryland 20850

Received May 12, 1999; Revised Manuscript Received June 30, 1999

ABSTRACT: *Escherichia coli* uracil DNA glycosylase (UDG) catalyzes the hydrolysis of premutagenic uracil bases in DNA by flipping the deoxyuridine from the DNA helix [Stivers, J. T., et al. (1999) *Biochemistry 38,* 952]. A general acid−base mechanism has been proposed whereby His187 facilitates leaving group departure by protonating the O2 of uracil and Asp64 activates a water molecule for nucleophilic attack at C1′ of the deoxyribose. Detailed kinetic studies on the H187Q, H187A, and D64N mutant enzymes indicate that Asp64 and His187 stabilize the chemical transition state by 5.3 and 4.8 kcal/mol, respectively, with little effect on substrate or product binding. The pH dependence of k_{cat} for wild-type and H187Q UDG indicates that an *unprotonated* group in the enzyme−substrate complex ($pK_a = 6.2 \pm 0.2$) is required for catalysis. This unprotonated group has a small ΔH of ionization (-0.4 ± 1.7 kcal/mol) and is absent in the pH profile for D64N UDG, suggesting that it corresponds to the general base Asp64. The pH dependence of k_{cat} for wild-type, H187Q, and D64N UDG shows no evidence for an essential *protonated* group over the pH range of 5.5−10. Hence, the pK_a of His187 must be outside this pH range if it serves as an electrophilic catalyst. These results support a mechanism in which Asp64 serves as the general base and His187 acts as a *neutral* electrophile, stabilizing a developing negative charge on uracil O2 in the transition state. In the following paper of this issue we establish by crystallography and heteronuclear NMR spectroscopy that the imidazole of His187 is neutral during the catalytic cycle of UDG.

The hydrolysis of the *N*-glycosidic bond in DNA is an important first step in the enzymatic repair of numerous types of damaged bases that arise spontaneously in DNA. Such base modifications, if left unrepaired, can lead to miscoding during replication of the genetic information or, alternatively, may result in cytotoxicity by blocking DNA replication or transcription (*1*). One frequent and unavoidable type of base modification is the loss of the exocyclic amino group of cytosine by simple hydrolysis, thereby resulting in a uracil base in DNA. A uracil base in double-stranded and single-stranded DNA is removed by the well-known and highly specific DNA repair enzyme uracil DNA glycosylase (UDG) (*2*).

UDG is an exceptional enzyme catalyst. It may be estimated that the catalytic rate enhancement of UDG is 10^{12} based on the solution rate of glycosidic bond hydrolysis in deoxyuridine extrapolated to pH 7 and 25 °C ($\sim 10^{-10}$ s^{-1}). Even more impressively, the affinity of the enzyme for its transition state is calculated to be 10^{-18} M.[1] These large factors make UDG one of the most proficient of enzyme catalysts and make it an attractive system to study the chemical basis for the enzymatic cleavage of the glycosidic bond in pyrimidine bases in DNA. Although much detailed and elegant work has been performed to understand the mechanism of glycosidic bond cleavage in several *purine N-ribo*hydrolase enzymes (*3*, *4*), little is known about the enzymatic mechanism of *N*-glycosidic bond hydrolysis of *pyrimidine deoxy*nucleotides in DNA.

It is not clear whether the mechanism of enzymatic glycosidic bond cleavage in pyrimidine and purine nucleotides will be the same because of the dramatically different acidities of the base leaving groups. A common catalytic feature in both solution and enzymatic catalysis of glycosidic bond hydrolysis in purine nucleosides is the protonation of the purine leaving group at N7 ($pK_a \sim 2$) (*3*−*5*). Indeed, the solution hydrolysis of purine nucleosides shows an apparent first-order dependence on proton concentration in the pH range ∼0−7, indicating that the protonated nucleoside is the reactive species for subsequent attack of water at C1′ (*6*). Similarly, several purine *N*-ribohydrolases have been suggested to proceed by an analogous mechanism involving preequilibrium protonation at N7 by a group on the enzyme (*3*, *4*). Both the enzymatic and nonenzymatic reactions of purine ribonucleosides are characterized by a transition state

† This work was supported by NIH Grant GM56834 (to J.T.S.). A.C.D. is a National Research Council Postdoctoral Research Associate.

* Address correspondence to this author: phone, 301-738-6264; fax, 301-738-6255; e-mail, stivers@carb.nist.gov.

[1] Catalytic power is defined as the rate of the enzymatic reaction (k_e) divided by the rate for the noncatalyzed reaction in solution (k_{non}). For UDG, $k_e = k_{max} = 150$ s^{-1}, where k_{max} is the single-turnover rate of glycosidic bond cleavage at 25 °C for optimal substrates (see text). The rate of nonenzymatic uracil hydrolysis at pH 7 extrapolated to the same temperature is $k_{non} \sim 10^{-10}$ s^{-1} (*7*, *8*). Therefore, the catalytic power is $150/10^{-10} = 10^{12}$-fold. Similarly, a lower limit estimate of the affinity of UDG for its transition state of $K_{TS} = 10^{-18}$ M may be obtained by dividing k_{non} by k_{cat}/K_m ($\sim 10^8$ M^{-1} s^{-1}).

10.1021/bi9910878 CCC: $18.00
Published on Web 09/14/1999

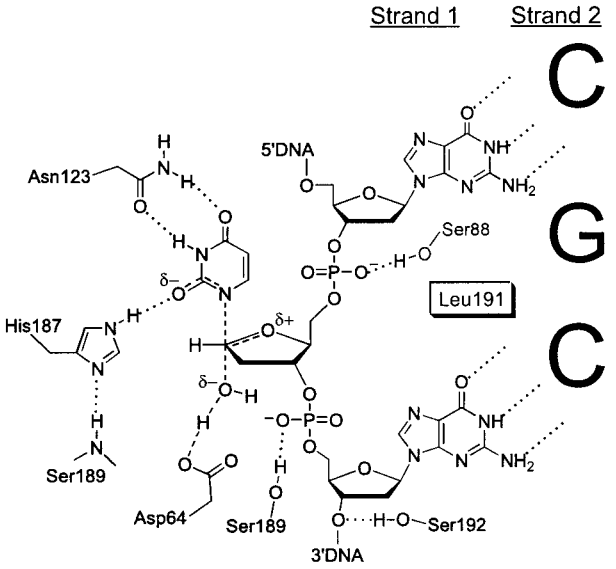

FIGURE 1: Schematic representation of the interactions in the transition state for glycosidic bond cleavage by uracil DNA glycosylase. Concerted electrophilic and general base catalysis by His187 and Asp64, respectively, is indicated. An oxycarbenium ion transition state is shown on the basis of chemical precedence, but this type of structure has not been established for UDG. The interactions are based on the crystal structures of free and uracil-bound *E. coli* UDG (*14*), as well as the human enzyme bound to the products abasic DNA and uracil (*10*, *13*). In these structures, the uracil forms the indicated hydrogen bonds to the completely conserved residues Asn123 and His187. The $N^{\delta 1}$ nitrogen of His187 is hydrogen bonded to the backbone amide of Ser189 in free *E. coli* UDG and the human UDG−product complex, providing structural evidence that His187 is neutral in its catalytically active state, a point established in the following paper. Key residues proposed to be involved in the uracil-flipping step are also shown (Ser189, Ser192, Ser88, and Leu191).

resembling an oxycarbenium ion, where a significant amount of positive charge develops on C1′ and O4′ (*7*).

In contrast to purine bases, thymidine and deoxyuridine glycosidic bond hydrolysis is pH *independent* in the pH range 2−8 and only shows catalysis by protons at pH values less than ∼2 (*8*, *9*). This is due to the extremely unfavorable equilibrium for protonation at O4 or O2, which have pK_a values ≤−3.4 (*9*). It is unknown to what extent the transition state structures for the pH-independent and acid-catalyzed reactions of pyrimidines differ and, if so, which transition state might resemble that of the enzymatic reaction. Thus, the thermodynamic and kinetic barriers to enzymatic hydrolysis of the *N*-glycosidic bond in a pyrimidine deoxynucleotide differ from those of a purine ribonucleoside, which suggests that the transition state structures and mechanisms of the two reactions could differ significantly. These questions make a detailed study of UDG of general mechanistic significance.

A plausible, yet unproved chemical mechanism for UDG has emerged, based on recent high-resolution crystal structures of the *Escherichia coli*, herpes virus, and human enzymes (Figure 1) (*10*−*14*). Structures of the human UDG bound to DNA have revealed that UDG flips the damaged base from the DNA helix using a phosphodiester "pinching" mechanism involving, at least in part, a trio of conserved serine residues (Figure 1). Recent structural and kinetic studies on the *E. coli* enzyme have shown that uracil flipping contributes less than 2 kcal/mol to specific DNA binding but contributes greatly to transition state stabilization by allowing the formation of key hydrogen bonds from the side chain atoms of Asn123 and His187 to uracil O4, H3, and O2 (*15*). In addition, rotation of the uracil base and sugar out of the DNA helix places C1′ in position for assisted attack by water. Although general base catalysis is not observed for the solution hydrolyses of the *N*-glycosidic bond of nucleosides (*8*), UDG apparently follows a different mechanism by deprotonating the incoming water nucleophile using the completely conserved residue Asp64 as the general base. Site-directed mutagenesis studies of the human enzyme support the structural evidence that His187 and Asp64 act as a general acid and base, respectively, because conversion of these groups to leucine and asparagine resulted in 300- and 2500-fold losses in activity (*11*). However, structural and mutagenesis data alone cannot establish the catalytic roles and ionization states of active site groups; thus other complementary approaches must be utilized to establish a chemical mechanism.

Here we report a detailed investigation of the roles of Asp64 and His187 in catalysis of glycosidic bond cleavage by UDG. The effects of these mutations on the pH dependencies of the kinetic parameters, uracil flipping, and substrate and product binding have been evaluated, allowing the determination of the interaction energies of these residues at each discrete step along the reaction pathway. The results indicate that Asp64 and His187 do not interact strongly with the flipped-out uracil in the enzyme−substrate complex or the bound uracil product. In contrast, Asp64 and His187 individually contribute about 5.3 and 4.8 kcal/mol to transition state stabilization, respectively. The pH dependencies of the kinetic parameters suggest that Asp64 has a high pK_a in the enzyme−substrate complex (pK_a = 6.2) and that His187 has a pK_a outside of the pH range 5−10 in both the free enzyme and the enzyme−substrate complex. In accord with the crystallographic and NMR studies presented in the following paper of this issue (*16*), a mechanism is proposed in which Asp64 acts as a general base and His187 serves as an electrophile by acting as a *neutral* hydrogen bond donor to uracil O2 in the transition state.

EXPERIMENTAL PROCEDURES[2]

Materials. Oligodeoxynucleotides were synthesized using an Applied Biosystems 390 synthesizer using standard phosphoramidite chemistry, except that the coupling times for addition of the fluorinated nucleoside phosphoramidites were increased to 10 min. All other nucleoside phosphoramidites were purchased from Applied Biosystems (Foster City, CA) or Glen Research (Sterling, VA). After synthesis

[2] Certain commercial equipment, instruments, and materials are identified in this paper in order to specify the experimental procedure. Such identification does not imply recommendation or endorsement by the National Institute of Standards and Technology, nor does it imply that the material or equipment identified is necessarily the best available for the purpose.

[3] Abbreviations: HPLC, high-performance liquid chromatography; UDG, *Escherichia coli* uracil DNA glycosylase; Tris-HCl, tris(hydroxymethyl)aminomethane hydrochloride; DSS, 2,2-dimethyl-2-silapentane-5-sulfonic acid; Hepes, 4-(2-hydroxyethyl)-1-piperazineethanesulfonic acid; SDS, sodium dodecyl sulfate; EDTA, (ethylenedinitrilo)tetraacetic acid, disodium salt; **P**, 2-aminopurine; U^{β}, β-isomer of 2′-fluoro-2′-deoxyuridine nucleotide; MALDI, matrix-assisted laser desorption−ionization mass spectrometry.

A

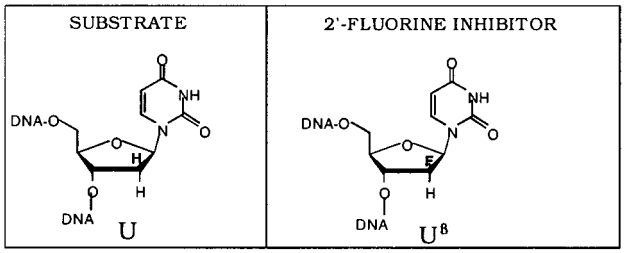

B

Abbreviation	Oligodeoxyribonucleotide
Duplex substrate	
AUA/TPT	5′GCGGCCAAAUAAAAAGCGC 3′ 3′CGCCGGTTT**P**TTTTTCGCG 5′
ssDNA substrates	
AUP-5	5′AUPAA 3′
pUPA	5′pUPA 3′
2′-U$^{\beta}$ inhibitors	
PU$^{\beta}$A/TGT	5′GCGGCCAA**P**U$^{\beta}$AAAAAGCGC 3′ 3′CGCCGGTTTG TTTTTCGCG 5′
AU$^{\beta}$A-5	5′AU$^{\beta}$AAA 3′
pU$^{\beta}$PA	5′pU$^{\beta}$PA 3′

FIGURE 2: Structures (A) and sequences (B) of the deoxyuridine DNA substrates and 2′-β-fluoro-2′-deoxyuridine substrate analogues (U$^{\beta}$) used in these studies. Abbreviation: **P**, 2-aminopurine deoxyribonucleotide.

and deprotection, the oligodeoxynucleotides were purified by anion-exchange HPLC[3] and desalted by gel filtration chromatography or reversed-phase HPLC. The size and purity of the DNA were assessed by denaturing polyacrylamide gel electrophoresis with visualization by ^{32}P radiolabeling or ethidium bromide staining. The concentrations were determined by UV absorption measurements at 260 nm, using the pairwise extinction coefficients for the constituent nucleotides (*17*). The oligodeoxynucleotides used in these studies are shown in Figure 2. Steady-state fluorescence emission spectra of the 2-AP-containing oligodeoxynucleotide samples were measured on a SPEX Fluoromax-2 spectrofluorometer.

5′-^{32}P End Labeling of Oligonucleotides. The uracil-containing strand of AUA/T**P**T (Figure 2) was 5′-^{32}P-end labeled using [γ-^{32}P]ATP in the presence of T4 polynucleotide kinase, the reaction was quenched by heating at 70 °C for 15 min, and the fractional incorporation of the label was determined by resolving the [γ-^{32}P]ATP from the oligonucleotide-bound radioactivity on a denaturing 20% mass fraction polyacrylamide gel, followed by scintillation counting of the excised bands. The unincorporated label was then removed from the quenched reaction using a membrane-based spin column (Qiagen, Chatsworth CA), and the purified DNA was dissolved in 2 mM Tris-HCl (pH 8.0) and 0.2 mM EDTA. The concentration of the DNA was determined by its specific activity.

Hybridization of Duplex DNA. Duplex DNA molecules (Figure 2) were hybridized from the respective single-strand oligonucleotides in TMN buffer (10 mM Tris-HCl, pH 8.0, 2.5 mM $MgCl_2$, 25 mM NaCl) or a buffer consisting of 20 mM Tris-HCl, pH 8.0, 60 mM NaCl, and 1 mM EDTA. Samples were heated to 70 °C followed by slow cooling to room temperature over at least 2 h. The duplexes were formed by using a 5−10% excess of the unlabeled strand such that all of the radiolabel (or 2-aminopurine-containing strand) was in the duplex form. This was confirmed by performing electrophoresis on a native 20% mass fraction polyacrylamide gel, followed by visualization using autoradiography or ethidium bromide staining.

Construction and Purification of Wild-Type and Mutated UDG Enzymes. UDG from *E. coli* strain B was cloned from *E. coli* strain B genomic DNA (Ultrapure, Sigma) using PCR. The full-length PCR product was ligated into the pET21a expression vector (Novagen, Madison WI) to give the pET21a-UDG construct, which was transformed into the *E. coli* expression strain BL21(DE3)plysS (Novagen) for protein expression. The enzyme was purified to >99% homogeneity as described (*14*, *18*). The concentration of the enzyme was determined using the relationship $\epsilon^{280} = 38\,511\ M^{-1}\ cm^{-1}$ (*19*). The D64N, H187Q, and H187A mutations were generated using the QuikChange double-stranded mutagenesis kit (Stratagene, La Jolla, CA). After the mutations in these constructs were confirmed by DNA sequencing of both strands, the mutated genes were cloned into the *Hin*dIII and *Nde*I sites of the pET28(a) expression vector (Novagen), which places a six histidine tag at the amino terminus. The pET28(H187Q), pET28(H187A), and pET28(D64N) constructs were then transformed into the recombination-deficient host BLR(DE3)plysS (Novagen). The mutated enzymes were purified using a nickel chelate resin according to the manufacturer's instructions (Qiagen). The use of this expression system ensured that the mutated enzymes were not contaminated with wild-type activity from the chromosomal copy of the UDG gene. [Control experiments established that the native UDG is not retained on the nickel resin (<0.0002% retention). Since expression of the chromosomal UDG is less than 1/1000 that of the mutated enzymes on the basis of activity measurements of soluble extracts, then the overall fractional contamination of the mutated enzyme preparations by wild-type UDG is about $1/10^8 = 1/[(1000)(10^5)]$. This level of contamination is 10^4-fold less than the damaging effects of these mutations on the activity of UDG and, therefore, cannot contribute to the measured activity of the mutated enzymes.] Controls also demonstrated that the histidine tag has little effect on the steady-state activity of the wild-type enzyme (see Table 1). The structural integrity of the H187Q or D64N enzymes was established either by high-resolution X-ray crystallography or by comparison of the backbone amide chemical shifts in $^1H-^{15}N$ HSQC spectra with that of the wild-type enzyme.

Dissociation Constant Determinations. The apparent dissociation constants (K_D^{app}) for two-step binding of UDG to the fluorescent DNA molecules **P**U$^{\beta}$A/TGT and pU$^{\beta}$**P**A (Figure 2) were determined by titrating fixed concentrations of the DNA with increasing amounts of UDG (*15*). The concentration of the DNA was set approximately equal to the K_D^{app} value for these experiments. An excitation wavelength of 320 nm was used to minimize background

Table 1: Kinetic and Thermodynamic Parameters and pK_a Values for Wild-Type *E. coli* UDG and Effects of D64N, H187Q, and H187A Mutations[a]

DNA or base	parameter	wt UDG	relative values[c] D64N	H187Q	H187A[b]
AUA/T**P**T	k_{cat} (s^{-1})	1.4 (1.2)	*9×10^{-3}*	*1.8×10^{-2}*	*5.0×10^{-3}*
	k_{cat}/K_m (μM^{-1} s^{-1})	47 (24)	*5.8×10^{-3}*	*2.1×10^{-2}*	*3×10^{-3}*
	K_m (μM)	0.03 (0.05)	*1.6*	*0.88*	*1.6*
	k_{max} (s^{-1})[d]	115	*3.8×10^{-4}*	*2.9×10^{-4}*	
AU**P**-5	k_{cat} (s^{-1})	21 (16)	*1.2×10^{-3}*	*3.1×10^{-3}*	*5.9×10^{-3}*
	k_{cat}/K_m (μM^{-1} s^{-1})	42 (15)	*1.4×10^{-3}*	*3.8×10^{-3}*	*6.6×10^{-3}*
	K_m (μM)	0.50 (1.1)	*0.84*	*0.80*	*0.87*
	k_{max} (s^{-1})[d]	157 (140)	*1.5×10^{-4}*	*3.3×10^{-4}*	
	pK_a[e]	6.2 ± 0.1		6.1 ± 0.2	
	pK_{a1}	5.7 ± 0.3	<6	<6	
	pK_{a2}	10.0 ± 0.3	>10	>10	
pU**P**A[f]	k_{cat} (s^{-1})	0.19	*1.0×10^{-3}*	*1.0×10^{-3}*	
	k_{cat}/K_m (μM^{-1} s^{-1})	0.15	*3.3×10^{-3}*	*1.4×10^{-3}*	
	K_m (μM)	1.3	*0.3*	*0.7*	
	k_{max} (s^{-1})[d]	0.24	*7.9×10^{-4}*	*7.9×10^{-4}*	
	pK_a[e]	6.6 ± 0.3			
	pK_{a1}	5.8 ± 0.2			
	pK_{a2}	8.1 ± 0.2			
PU$^{\beta}$A/TGT	K_D^{app} (μM)[g]	0.05	*1.2*	*1.1*	
AU$^{\beta}$A-5	K_D^{app} (μM)	0.22	*0.36*	*0.95*	
pU$^{\beta}$**P**A	K_D^{app} (μM)	2.1	*0.49*	*1.5*	
uracil	K_D (μM)	96	*0.53*	*1.99*	

[a] $T = 25$ °C, TMN buffer (pH = 8.0). The kinetic measurements for the mutated enzymes were determined using the amino-terminal 6× histidine tag constructs (see Experimental Procedures). The K_D measurements were performed on the native mutant enzymes without the 6× histidine tag. The kinetic parameters for the wild-type enzyme were determined for the native enzyme and the 6× His tag construct (values in parentheses). Errors are ≤10% for k_{cat} and ≤20% for K_m unless otherwise noted. [b] The error in the K_m value for AUA/T**P**T using H187Q UDG is ±40%. [c] The damaging effects of the mutation on the indicated parameter relative to wild-type UDG are shown in italics (i.e., relative effect = 6× His tag mutant activity/6× His tag wt UDG activity, except as noted for the K_D and pU**P**A kinetic measurements). [d] The single-turnover k_{max} value is the concentration-independent maximal single-turnover rate (see Figure 5 and Experimental Procedures). [e] These pK_a values are defined in eqs 4 and 5 (see Experimental Procedures). [f] For pU**P**A, the K_m values for the mutated enzymes have 50−60% errors due to the very slow rates at low [S]. The damaging effects for this substrate are reported relative to the native wild-type UDG. [g] K_D^{app} is the apparent dissociation constant for two-step binding to form the base-flipped species (*15*).

fluorescence from tryptophan residues of the enzyme, and 2-AP emission spectra in the range 340−450 nm were collected. The binding data were fitted to eq 1 after the

$$F = F_o - \{(F_o - F_f)[DNA]_{tot}/2\}\{b - (b^2 - 4[UDG]_{tot}[DNA]_{tot})^{1/2}\} \quad (1)$$

$$b = K_D^{app} + [UDG]_{tot} + [DNA]_{tot}$$

background fluorescence of UDG was subtracted from each spectrum (F_o and F_f are the initial and final fluorescence intensities, respectively).

The dissociation constants for the uracil product and the nonfluorescent AU$^{\beta}$A-5 substrate analogue were determined by competitive displacement of the fluorescent pU$^{\beta}$**P**A from UDG. The fluorescence emission intensities at 370 nm as a function of total added ligand concentration were fit with the computer program DynaFit, using the known dissociation constant for pU$^{\beta}$**P**A and the chemical equations for competitive binding of two ligands to a single site (*20*).

Steady-State Kinetic Measurements. Uracil glycosidic bond cleavage in duplex DNA was monitored continuously at 25 °C in a buffer (TMN) consisting of 10 mM Tris-HCl, pH 8.0, 2.5 mM $MgCl_2$, and 25 mM NaCl. A continuous kinetic assay was used which monitored the fluorescence increase of a 2-aminopurine base (**P**) that was either base paired with or located adjacent to the excised uracil (see DNA sequences in Figure 2) (*15*, *18*). The steady-state kinetic parameters k_{cat} and k_{cat}/K_m were obtained from plots of the observed rate constants (k_{obsd}) against substrate concentration ($[S]_{tot}$) using a standard hyperbolic kinetic expression and the program Grafit 4 (*21*) according to eqs 2 and 3. In eq 2, $\Delta F/\Delta t$ is the

$$k_{obsd} = (1/\Delta a)(\Delta F/\Delta t)(1/[UDG]_{tot}) \quad (2)$$

$$\Delta a = \Delta F_{tot}/[S]_{tot}$$

$$k_{obsd} = k_{cat}/(K_m + [S]) \quad (3)$$

initial rate in fluorescence units per second, ΔF_{tot} is the total fluorescence increase for 100% conversion of a given substrate concentration ($[S]_{tot}$) to product, and $[UDG]_{tot}$ is the total UDG concentration. The values for Δa were determined either by letting the reaction go to completion or by adding 10−20 nM UDG to rapidly bring the reaction to its end point after completing the initial rate measurements. For the time−base scans, an excitation wavelength of 310 or 320 nm was used, the emission was observed at 370 nm, and sampling was at intervals of 1 s.

Rapid Chemical Quench-Flow Single-Turnover Kinetic Measurements. Experiments were performed on a three-syringe apparatus (KinTek RQF-3, University Park, PA) at 25 °C in TEN buffer (10 mM Tris-HCl, pH 8.0, 60 μM NaCl, 1 mM EDTA) with excess UDG (10 μM final concentration) and limiting amounts (10−20 nM) of the 5′-^{32}P-end-labeled

duplex DNA substrates AUA/T**P**T. Reactions were initiated by mixing equal volumes (~30 μL) of the labeled substrate and enzyme solutions. At time points between 0 and 50 ms, the reactions were quenched with 1 M HCl delivered from the quench syringe. (Identical reaction kinetics were observed using 0.5 M HCl, thus confirming the effectiveness of the quench.) The samples (15) were collected in 5 mL polyethylene tubes and immediately 100 μL of phenol/chloroform/isoamyl alcohol (25:24:1 volume ratio) was added to denature the enzyme. The samples were vortexed vigorously, and 40 μL of 3 M Tris base was added to adjust the pH to between 7 and 8 to prevent decomposition of the DNA under acidic conditions. A 10 μL sample of each reaction was mixed with 10 μL of loading buffer (95% volume ratio formamide, 0.05% mass fraction bromophenol blue, 0.05% mass fraction xylene cyanol), heated at 90 °C for 2 h to thermally cleave the abasic sites generated by the *N*-glycosylase reaction, and analyzed by electrophoresis (40 V/cm on a 20% mass fraction polyacrylamide gel containing 8 M urea). The fraction of the total radioactivity in the substrate and β-elimination product bands at each time point was then quantified using a Molecular Dynamics Storm 840 phosphorimager. The data were fitted to a first-order rate equation using the computer program Grafit 4 (*21*). The reported rate constants (k_{max}) are independent of the enzyme concentration (not shown) and reflect a single turnover of the enzyme−substrate complex.

The single-turnover kinetics for the substrates pU**P**A and AU**P**-5 were measured in stopped-flow fluorescence experiments by following the increase in 2-AP fluorescence resulting from glycosidic bond cleavage. Stopped-flow fluorescence experiments were performed at 25 °C in TMN buffer using an Applied Photophysics device in the two syringe mode (dead time = 1.1 ms). The 2-aminopurine-containing DNA was excited at 310 nm, and the fluorescence emission was monitored using a 360 nm cut-on filter. The data were fitted as a first-order process ($F_t = \Delta F e^{-k_{max}t} + C$, where F_t is the fluorescence at time t, ΔF is the total amplitude of the fluorescence change, k_{max} is the single-turnover rate constant, and C is a constant offset).

pH Dependence of Catalysis. For wild-type UDG, the pH dependencies of the rate of glycosidic bond cleavage for substrates pU**P**A and AU**P**-5 were determined using the fluorescence assay in the pH range 4.6−10 at 25 °C with the following buffers (all 10 mM): sodium acetate, pH 4.6−5; NaMES, pH 5.0−6.5; NaHEPES, pH 6.5−7.5; Tris-HCl, pH 7.5−8.5; NaCHES, pH 8.5−9.5; NaCAPS, pH 9.5−10. The [$MgCl_2$] was 2.5 mM, and the [NaCl] was adjusted to maintain the ionic strength at 0.03 M. Initial rates and the kinetic parameters were determined as described above. The values for Δa (eq 1) were found to be pH dependent and were determined at each pH value. The pH dependencies of k_{cat} and k_{cat}/K_m were fitted to eqs 4 and 5, respectively, by nonlinear regression analysis using Grafit 4 (*21*).

$$k_{cat} = \frac{(k_{cat})^{max}}{1 + [H^+]/K_a} \quad (4)$$

$$k_{cat}/K_m = \frac{(k_{cat}/K_m)^{max}}{1 + [H^+]/K_{a1} + K_{a2}/[H^+]} \quad (5)$$

For the H187Q and D64N enzymes, the pH dependencies of k_{cat} and k_{cat}/K_m were determined by measuring the reaction velocities at AU**P**-5 substrate concentrations 10-fold greater than or less than the K_m value at neutral pH, respectively. This approach makes the assumptions that the observed reaction rate is (i) independent of substrate concentration for [S] $\geq 10K_m$ and (ii) linear in substrate concentration for [S] $\leq 10K_m$. These assumptions were directly tested by varying the substrate concentrations by 2-fold at the pH values where rate decreases were observed.

Solvent Deuterium Isotope Effect on k_{cat}. The solvent deuterium isotope effect on k_{cat} for wild-type UDG was determined at 25 °C using the slow substrate pU**P**A to minimize the reverse commitment to catalysis, which would be expected to mask any intrinsic isotope effect for a good substrate such as AU**P**-5. Tris buffers (10 mM, $pH^{app} = 8.0$) in H_2O and D_2O (99.9 atom % D) were prepared by mixing together gravimetrically prepared solutions of 1 M Tris-LCl (L = H or D) and 1 M Tris base to give the desired final pH. Prior to preparing the D_2O buffers, the acid and base components had been lyophilized to dryness and redissolved in D_2O three times to remove any exchangeable protons. The final reaction buffers also contained 2.5 mM $MgCl_2$ and 20 mM NaCl. The UDG and AU**P**-5 stocks were prepared in D_2O and H_2O buffers, respectively. The contribution of protons from the AU**P**-5 stock to the D_2O reaction was negligible (~1 atom % H) and was ignored in the calculation of the isotope effect. The isotope effect measurement (k_{H_2O}/k_{D_2O}) was repeated three times and the mean value and standard deviation were calculated.

pH Titration of Uracil H3 in pUPA by ^{1}H NMR. One-dimensional proton NMR experiments were performed at 25 °C with a Bruker Avance 500 MHz NMR spectrometer. The sample included 0.14 mM pU**P**A (0.13 mM), 10 mM NaH_2PO_4, and 25 mM NaCl in 0.25 mL of 95% H_2O and 5% D_2O. The spectra were recorded with the following acquisition parameters: a spectral width of 5000 Hz, the carrier frequency set at 4.772 ppm relative to internal DSS, an acquisition time of 0.82 s, and a relaxation delay of 0.5 s. FIDS of 4K complex points were processed by zero-filling to 16K data points and applying 2.0 Hz line broadening. Titrations were performed by the addition of small aliquots of NaOH. The pK_a value for uracil H3 in pU**P**A was determined by following the chemical shift changes (δ) in the uracil H5 and H6 proton resonances as a function of pH. The titration data were fitted by nonlinear regression analysis to eq 6, where δ_1 and δ_2 are the limiting chemical shifts at low and high pH, respectively.

$$\delta\ (ppm) = \frac{\delta_1 + \delta_2(10^{pH-pK_a})}{10^{pH-pK_a} + 1} \quad (6)$$

Propagation of Errors. For all the kinetic and thermodynamic parameters we report standard uncertainties of the theoretical fits, assuming that the uncertainties in the individual measurements are approximated by the standard uncertainty of the points from the fitted curve.

RESULTS

Mutational Effects on Substrate Analogue and Uracil Binding. We recently developed a convenient fluorescence-

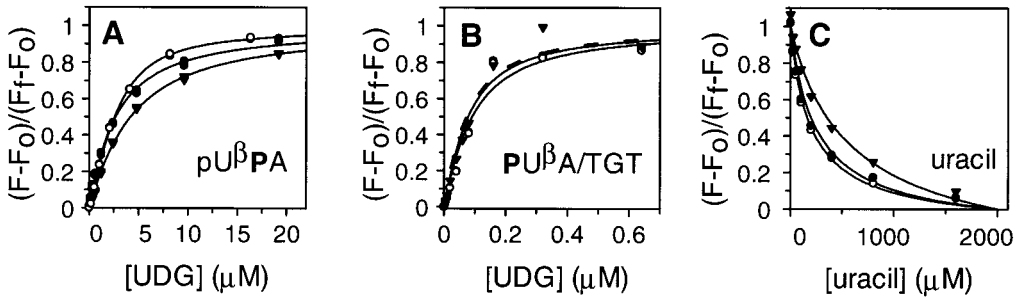

FIGURE 3: Determination of the effects of the D64N and H187Q mutations on the binding affinity of substrates and products of the UDG reaction. (A, B) Measurement of the dissociation constants for (A) pU$^{\beta}$**P**A and (B) **P**U$^{\beta}$A/TGT. The fractional fluorescence change as a function of total [UDG] is plotted for wild-type (closed circles), H187Q (triangles), and D64N UDG (open circles). (C) Measurement of the dissociation constant for uracil using a competitive fluorescence displacement assay. Increasing concentrations of uracil (0−1.6 mM) were added to a preformed complex of pU$^{\beta}$**P**A with each enzyme (symbols as in panels A and B).

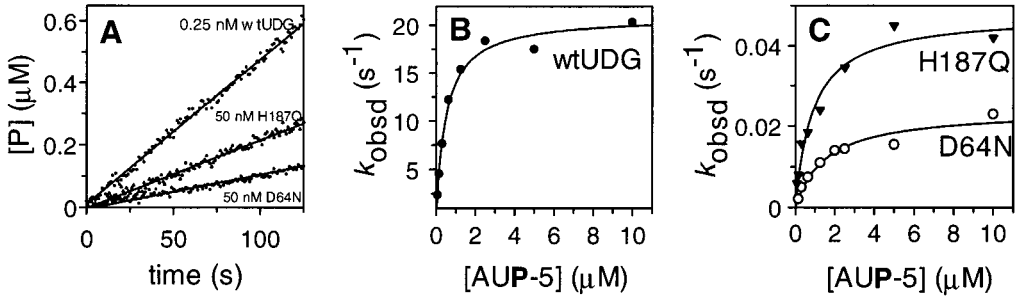

FIGURE 4: Determination of the effects of the D64N and H187Q mutations on the steady-state kinetics of the UDG reaction. (A) Typical initial rate measurements using the 2-aminopurine-based continuous kinetic assay (AU**P**-5 concentration = 10 μM; note that the enzyme concentration is 400-fold greater for the mutant enzymes as compared to wild-type UDG). Hyperbolic saturation curve for the reaction of AU**P**-5 with (B) wild-type UDG and (C) D64N and H187Q UDG. The initial rate of product formation was calculated according to eq 2.

based assay to measure the binding of stable 2′-β-fluoro-2′-deoxyuridine (U$^{\beta}$) substrate analogues to UDG (*15*, *18*). This assay relies on the fluorescence changes of a 2-aminopurine (**P**) reporter nucleotide that is placed adjacent to the U$^{\beta}$ nucleotide in single-strand or duplex DNA (see Figure 2). For such DNA, a 3−8-fold increase in the **P** fluorescence results when the U$^{\beta}$ flips into the UDG active site due to a decrease in base stacking interactions that otherwise strongly quench **P** fluorescence (*15*). This useful assay can also be used in a competition mode to determine the binding constants of nonfluorescent ligands such as uracil and AU$^{\beta}$A-5.

Direct and competitive binding studies on the wild-type and mutant enzymes were performed to assess the energetic contributions of the imidazole and carboxylic acid side chains of His187 and Asp64 to the binding of single- and double-stranded uracil-containing DNA and free uracil (Figure 3, Table 1). Representative direct binding experiments for the duplex substrate analogue **P**U$^{\beta}$A/TGT and the short single-strand substrate analogue pU$^{\beta}$**P**A are shown in panels A and B of Figure 3, respectively. The binding constants for **P**U$^{\beta}$A/TGT and pU$^{\beta}$**P**A are 0.05 μM and 2.1 μM, respectively, for wild-type UDG. The binding constants for the D64N and H187Q mutants differ by less than 2-fold as compared to the wild-type values, indicating that these residues do not contribute significantly to stabilization of the enzyme−substrate complex (Table 1). Likewise, the wild-type, D64N, and H187Q enzymes have similar dissociation constants for uracil in the range of 50−190 μM (Figure 3D). The affinity of wild-type UDG for uracil (K_D = 96 μM) agrees well with the K_I of 120 μM previously determined for noncompetitive inhibition of UDG by uracil (*19*). Similar binding measurements for the H187A enzyme were not possible because it expressed very poorly in our hands, yielding small amounts protein after purification. Nevertheless, enough of the H187A enzyme was obtained to measure steady-state K_m values for the substrates AUA/T**P**T and AU**P**-5, which showed that the alanine mutation, like glutamine, has little effect on the binding of uracil-containing DNA (see below and Table 1).

Mutational Effects on the Steady-State Kinetic Parameters of UDG. The steady-state kinetic parameters for the enzymes were determined using the continuous 2-aminopurine fluorescence assay for glycosidic bond cleavage recently developed in our laboratory (*18*). This assay takes advantage of the large fluorescence increase that results from the enzymatic creation of an abasic site adjacent or opposite to a fluorescent 2-aminopurine reporter group (**P**) in the substrate DNA (*15*, *18*).

Typical initial rate data and Michaelis−Menten plots for the reaction of the fast substrate AU**P**-5 with wild-type, H187Q, and D64N UDG are shown in Figure 4, and the kinetic parameters for the AUA/T**P**T, AU**P**-5, and pU**P**A substrates are reported in Table 1. For wild-type UDG, the k_{cat} = 20 s^{-1} for AU**P**-5 is about 15-fold greater than the k_{cat} for the duplex substrate AUA/T**P**T, but the k_{cat}/K_m values are essentially diffusion controlled for both substrates ($\sim 10^8$ M^{-1} s^{-1}). This 15-fold greater k_{cat} value for AU**P**-5 as compared to AUA/T**P**T is due to a kinetic difference in a rate-limiting step after bond cleavage, because these substrates have similar single-turnover glycosidic bond cleavage rates (see below). The k_{cat} = 0.19 s^{-1} and k_{cat}/K_m = 0.15 μM^{-1} s^{-1} for the slow trinucleotide substrate pU**P**A are 110- and 280-fold less than for AU**P**-5, respectively, and the K_m = 1.3 μM for pU**P**A is similar to the K_D = 2.1 μM for the substrate analogue pU$^{\beta}$**P**A. Thus, pU**P**A is a slow substrate that follows a rapid equilibrium binding mechanism. The

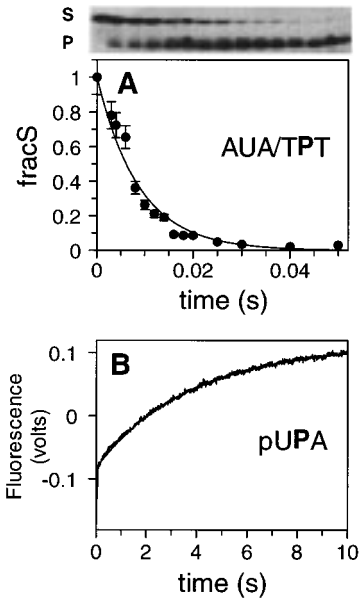

FIGURE 5: Single-turnover kinetics of the UDG reaction. (A) Reaction of 5′-^{32}P-labeled AUA/T**P**T (20 nM) with 10 μM wild-type UDG as measured by chemical quench-flow methods using the piperidine-induced abasic site cleavage assay. The line is the best fit to a first-order decay process (k_{max} = 115 ± 5 s^{-1}). (B) Reaction of pU**P**A (250 nM) with 10 μM UDG as measured in a stopped-flow fluorescence experiment (k_{max} = 0.24 ± 0.01 s^{-1}; see Table 1).

110-fold difference in k_{cat} between AU**P**-5 and pU**P**A is similar to the 100-fold difference previously reported for pT$_5$-UT$_5$ and pUTT (*22*). As shown in the crystal structure of human UDG bound to DNA, the faster rate for the longer substrate AU**P**-5 can be attributed to key interactions of the enzyme with phosphodiester groups that are not present in the shorter pU**P**A substrate (*10*).

In general, the effect of the H187Q mutation is to lower k_{cat} by about 60-, 300-, or 1000-fold depending on whether the substrate is AUA/T**P**T, AU**P**-5, or pU**P**A, respectively (Table 1). The kinetic behavior of the H187A enzyme is similar to H187Q UDG (Table 1). This indicates that the side chain hydrogen-bonding groups of Gln187, which are not present in H187A UDG, do not provide additional binding interactions with the substrate, transition state, or product. The structural basis for this unexpected result is revealed by the crystal structure of the H187Q UDG−uracil complex, which shows that the Gln187 side chain is positioned such that it cannot hydrogen bond with the uracil base (*16*). The D64N mutation is found to be somewhat more damaging than the H187Q mutation and lowers k_{cat} by 100-, 830-, and 1000-fold for AUA/T**P**T, AU**P**-5, and pU**P**A, respectively (Table 1). Consistent with the binding studies using stable substrate analogues, none of these mutations has a significant effect on K_m (≤2-fold), indicating that His187 and Asp64 act to selectively stabilize the transition state.

Steady-State Kinetic Studies Do Not Measure Maximal Mutational Effects. In general, mutational effects will be underestimated if product release is rate limiting for the wild-type enzyme and another step such as the chemical step is rate limiting for mutant enzymes.[4] To examine whether maximal mutational effects were being measured for UDG, we also determined the mutational effects on the single-turnover rate (k_{max}). The ratio of the single-turnover rate to k_{cat} (k_{max}/k_{cat}) provides a measure of the extent to which product release is rate limiting for a given substrate or enzyme variant. Thus, a large k_{max}/k_{cat} ratio indicates that a slow step after the chemistry step is rate limiting for k_{cat}, while a k_{max}/k_{cat} ratio of unity indicates that the chemistry step is rate limiting.

For wild-type UDG, the single-turnover rapid chemical quench-flow experiment using AUA/T**P**T shows that the glycosidic bond is cleaved with a k_{max} = 115 s^{-1}, which is ~80 times faster than the subsequent step that limits the k_{cat} value for this substrate (see Figure 5A and Table 1). A similar k_{max} of 140 s^{-1} was determined in a stopped-flow fluorescence experiment using AU**P**-5 (not shown), and this value is about 6-fold greater than the k_{cat} for this substrate (Table 1). The k_{max}/k_{cat} ratios of 6 and 80 for AU**P**-5 and AUA/T**P**T, respectively, suggest that product release is rate limiting for both of these substrates. In contrast, the k_{max}/k_{cat} ratio for the slow substrate pU**P**A is 1.3 ± 0.1, indicating that for this substrate the chemical step is rate limiting under steady-state or single-turnover conditions using wild-type UDG (Figure 5B, Table 1).

For the mutant enzymes, the k_{max}/k_{cat} ratio is near unity for AUA/T**P**T, AU**P**-5, and pU**P**A, indicating that the chemical step is rate limiting regardless of the substrate (see k_{cat} and k_{max} values in Table 1). Accordingly, the mutational effects measured by single-turnover experiments ($k_{max}^{mut}/k_{max}^{wt}$) are greater than those measured by steady-state experiments ($k_{cat}^{mut}/k_{cat}^{wt}$) by about 7- and 60-fold using AU**P**-5 and AUA/T**P**T, respectively. This is quantitatively explained by the observation that, for the wild-type enzyme, a step leading to product release is 6- and 80-fold slower than glycosidic bond cleavage for these respective substrates (see above). This analysis indicates that the mutational effects on the steady-state kinetic parameters are diminished by differing amounts, depending on the extent to which the product release step is rate limiting for the wild-type enzyme with a given substrate.

Identification of Group pK_a Values Involved in Catalysis. The above kinetic results show that AU**P**-5 is a diffusion-controlled substrate (k_{cat}/K_m = 42 μM^{-1} s^{-1}) and that the rate-limiting step using k_{cat} conditions is not the chemistry step. For such a substrate, the pH dependence of the kinetic parameters may not be described by a simple ionization curve, and the *apparent* pK_a values may be shifted to lower or higher values than the *true* pK_a values determined with a slow substrate that reacts by a rapid equilibrium mechanism (see ref *23* and references therein). Thus, to be confident of the pK_a values for wild-type UDG, we determined the pH dependence of the kinetic parameters using AU**P**-5 and pU**P**A (Figure 6A,B).

The pH dependencies of k_{cat} for AU**P**-5 and pU**P**A show the requirement for a single basic group in the enzyme−substrate complex with a pK_a of 6.2 ± 0.2 and 6.6 ± 0.3, respectively (eq 4, Table 1). These results provide excellent

[4] This point can be easily appreciated from the kinetic expression $k_{cat} = k_{max}k_{off}/(k_{max} + k_{off})$, which holds for the simple mechanism:

$$ES \xrightarrow{k_{max}} EP \xrightarrow{k_{off}} E + P$$

Thus, assuming $k_{max}^{mut}/k_{max}^{wt}$ = 1/1000, and $k_{off}^{wt} = k_{off}^{mut}$ = 1/100 k_{max}^{wt}, then the damaging effect on $k_{cat} = k_{cat}^{mut}/k_{cat}^{wt}$ = 1/10 would be 100-fold less than the effect on the chemical step (k_{max}).

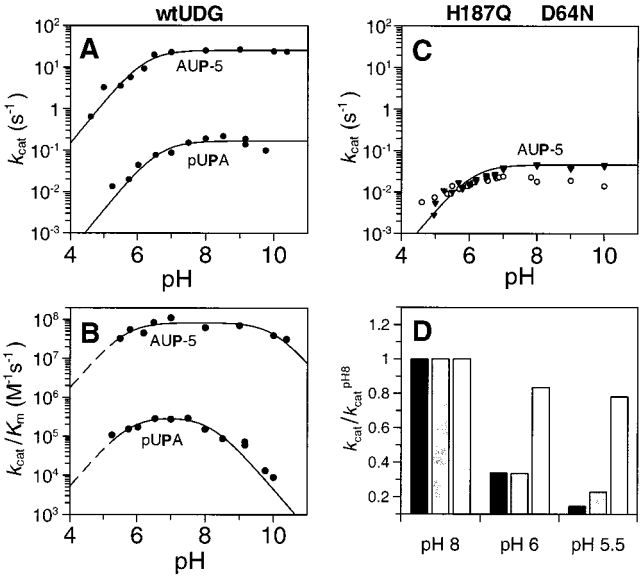

FIGURE 6: pH dependence of the steady-state kinetic parameters for wild-type UDG and the H187Q and D64N mutant enzymes. pH dependence of (A) k_{cat} and (B) k_{cat}/K_m for wild-type UDG for the fast substrate AU**P**-5 and the slow substrate pU**P**A (see text). The curves are best fits to eqs 4 and 5 using the pK_a values reported in Table 1. (C) pH dependence of k_{cat} for H187Q (triangles) and D64N UDG (open circles) using AU**P**-5. No curve is drawn for the D64N enzyme because the data did not fit the equation for a single essential pK_a. (D) Relative k_{cat} values as a function of pH for the wild-type (black), H187Q (gray), and D64N (open) enzymes normalized to their values at pH 8.0 (S = AU**P**-5). This plot more clearly demonstrates the smaller pH dependence of the reaction catalyzed by D64N UDG (see text).

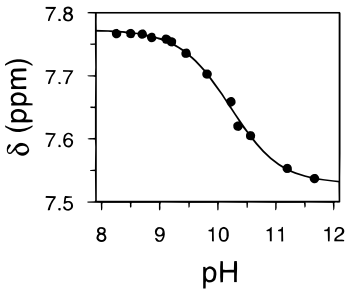

FIGURE 7: Determination of the pK_a for uracil N3 in the substrate pU**P**A using ^{1}H NMR spectroscopy. The chemical shift of the resolved H5 proton of the uracil base ($J_{H5,H6}$ = 7.5 Hz) was followed as a function of pH, and the solid line is the best fit to eq 6 (pK_a = 10.2 ± 0.03). This pK_a is similar to the pK_a of N3 in uridine 5′-monophosphate but two units higher than the upper pK_a seen in the pH dependence of k_{cat}/K_m for this substrate (Figure 6B).

evidence that the AU**P**-5 and pU**P**A substrates utilize the same mechanism and that the slower reactivity of pU**P**A is not due to its inability to interact with this essential active site group. The similarity of these pK_a values for a fast and slow substrate suggests that true pK_a values for the enzyme−substrate complex are being measured. In addition, these results provide no evidence for an essential acidic group in the enzyme−substrate complex in the pH range ∼5−10 (Figure 6A). Thus, if general acid catalysis by His187 is occurring, its pK_a is outside of this range. This result is consistent with the NMR results reported in the following paper (*16*), which show that His187 is neutral in the UDG−pU$^{\beta}$**P**A complex at pH 6.8.

For AU**P**-5, a very broad bell-shaped dependence of k_{cat}/K_m on pH is observed (Figure 6B). The data may be fitted to eq 5, which suggests that an unprotonated group with a pK_{a1} = 5.7 and a protonated group with a pK_{a2} = 10.0 on the free enzyme or substrate are required for catalysis. The pK_{a1} may be attributed to the same group seen in the pH dependence of k_{cat}, suggesting that this pK_a is shifted upward by ∼0.5 unit upon AU**P**-5 binding. However, as shown below and in the following paper, the upper pK_a of 10 for AU**P**-5 cannot be due to ionization of His187 in the free enzyme and may instead be due to the ionization of uracil N3 in the substrate (see below).

For pU**P**A, a much narrower bell-shaped profile is observed for the pH dependence of k_{cat}/K_m as compared to AU**P**-5, with pK_a values of 5.8 and 8.1 on the ascending and descending limbs, respectively (Figure 6B). The lower pK_a is indistinguishable from that observed for AU**P**-5 (Table 1), but the upper pK_a of 8.1 is not observed for AU**P**-5 using the wild-type, H187Q, or D64N enzymes (see below). We considered the possibility that this pK_a may reflect general acid catalysis by His187 or a perturbed pK_a for uracil N3 in pU**P**A. However, the pK_a of His187 is <5.0, as shown in the following paper of this issue (*16*), and a pK_a of 10.2 for uracil N3 in pU**P**A was determined by ^{1}H NMR (Figure 7), which is similar to the pK_a of 10.1 for N3 in uridine 5′-monophosphate (*24*). We speculate that this pK_{a2} = 8.1 results from either (i) an abnormally high pK_a for the 5′-phosphate monoester group of pU**P**A, with the dianion binding much more weakly than the monoanion form, or (ii) an interaction between the dianion and a cationic group on the enzyme.

pH−Rate Studies of H187Q and D64N UDG. The k_{cat} for H187Q UDG shows essentially the same pH dependence as the wild-type enzyme, establishing that the pK_a = 6.2 for the wild-type enzyme is not due to titration of His187 (Figure 6C, triangles). In contrast, the k_{cat} for D64N UDG shows only a 20% decrease from pH 8.0 to pH 5.5, suggesting that the essential pK_a in the enzyme−substrate complex for the wild-type and H187Q enzymes is due to titration of Asp64 (Figure 6C, open circles). The significantly different pH dependence of the D64N enzyme as compared to the wild-type and H187Q enzymes is shown more clearly in the linear scale bar graph in Figure 6D, where the observed k_{cat} values at pH 8.0, 6.0, and 5.5 are normalized to the values at pH 8.0. Similar to wild-type UDG, a very broad pH dependence of k_{cat}/K_m was observed for both H187Q and D64N UDG (not shown). As a result, only lower and upper limit pK_a values of ≤6 and ≥10 for k_{cat}/K_m are reported in Table 1.

To provide further evidence that the basic group in the enzyme−substrate complex is due to ionization of an essential carboxylic acid group, we measured the temperature dependence of this pK_a in the temperature range 5−35 °C (Figure 8). This approach is based on the fact that carboxylic acids have small enthalpies of ionization (ΔH_{ion} = ±1.5 kcal/mol), while imidazole, sulfhydryl, and amino groups have much larger values in the range 6−13 kcal/mol (*25*). The measured ΔH_{ion} = −0.4 ± 1.0 kcal/mol is well outside the range expected for an imidazole, sulfhydryl, or amino group and supports the suggestion that the pK_a of 6.2 in the enzyme−substrate complex is due to the ionization of the general base, Asp64.

Solvent Deuterium Kinetic Isotope Effect on k_{cat}. The solvent deuterium isotope effect on k_{cat} was measured to

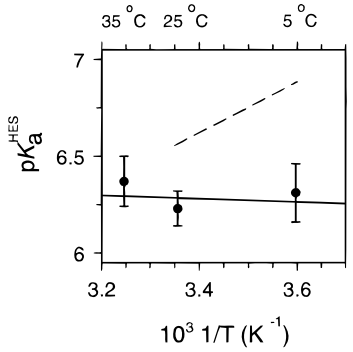

FIGURE 8: Temperature dependence of the essential pK_a in the enzyme−substrate complex. The slope of the solid line corresponds to an ionization enthalpy of -0.4 ± 1.7 kcal/mol. The dashed line shows the *minimum* slope expected for ionization of an imidazole, sulfhydryl, or amino group ($\Delta H_{ion} = 6-13$ kcal/mol).

determine whether a proton bridge exists between the H^{ϵ_2} imidazole proton of His187 and uracil O2 in the transition state. Such an interaction could form a low-barrier hydrogen bond, which should be manifested as a 2.5−5-fold slower k_{cat} in D_2O as compared to H_2O (*26*). The measured $k_{cat}^{H_2O}/k_{cat}^{D_2O} = 0.78 \pm 0.05$ ($n = 3$) using pU**P**A provides no evidence for such an interaction. The slightly faster rate in D_2O, which is reproducible with this substrate, is impossible to interpret in detail but could result from medium effects or the effects of solvent on conformational changes in UDG. We note that this small inverse effect is not likely due to the enzyme being in different ionization states in the two isotopic solvents, because the measurements were made in the pH-independent region of the pL rate profiles (L = H or D).

DISCUSSION

Energetic Contributions of His187 and Asp64 to DNA Binding, Uracil Flipping, and Catalysis. The goal of any mutational analysis of an enzyme is to quantify the energetic contributions of amino acid side chains to the binding of the substrate, products, or the transition state. The stable substrate analogues and fluorescence methods we have developed to study the UDG reaction provide a unique opportunity to quantify the interactions of the Asp64 and His187 side chains at discrete steps on the reaction pathway. The 2′-U$^{\beta}$-DNA binding experiments indicate that Asp64 and His187 contribute less than 0.4 kcal/mol toward stabilization of the flipped-out uracil base in the substrate and do not significantly change the affinity of UDG for the uracil product ($\Delta\Delta G \leq 0.4$ kcal/mol). In contrast, the H187Q and D64N mutations decrease the single-turnover k_{max} by as much as 3500- and 6600-fold, corresponding to a 4.8 and 5.3 kcal/mol destabilization of the transition state. Thus, it may be concluded that these residues interact weakly with the substrate or product but strongly with the transition state (see Figure 7 in the following paper of this issue).

The above energetic considerations lead to a picture of the reaction pathway in which the enzyme binds relatively loosely to the flipped-out uracil nucleotide ($K_D^{app} = 80-150$ nM) and then tightens its grip on the uracil base and sugar, leading to a transition state that is bound about 10^{12}-fold more tightly than the ground state ($K_{TS} = 10^{-18}$ M).[1] Finally, the enzyme "relaxes" to form loosely bound products. Such differential binding of the substrate, transition state, and products may be driven by subtle conformational changes in UDG. Direct evidence for conformational changes in the substrate and enzyme before *and* after glycosidic bond cleavage has been provided by stopped-flow fluorescence studies of *E. coli* UDG (*15*) and crystallographic studies of the human enzyme (*10*). In addition, significant differences are observed in the $^1H-^{15}N$ HSQC chemical shift patterns of uniformly ^{15}N-labeled UDG bound to the substrate analogue AU$^{\beta}$**P**-5, as compared to the products, abasic DNA and uracil (not shown). Thus taken together, the mutagenesis, kinetic, and structural data indicate compression and relaxation of the enzyme before and after the chemical step.

Roles of Asp64 and His187 in the Chemical Mechanism of Glycosidic Bond Hydrolysis. The essential pK_a of 6.2 in the enzyme−substrate complex for the wild-type enzyme, its absence in the D64N enzyme, and the small temperature dependence of this pK_a support the structural and mutagenesis evidence implicating Asp64 as the general base catalyst (see Figures 6 and 7). An alternative mechanism in which Asp64 acts as a nucleophile by direct attack at C1′ is unlikely because (i) mutation of nucleophilic residues typically results in catalytic losses of $>10^5$-fold (*27*−*29*) and (ii) recent structures of the human enzyme bound to product abasic DNA and uracil show that the C1′ hydroxyl group is in the α configuration as expected for a general base mechanism (*10*). An essential Asp residue is observed in the active sites of many DNA glycosidases and *N*-ribohydrolases, suggesting that an analogous general base mechanism is followed for these related enzymes (*30*, *31*).

The structural and mutagenesis studies also indicate an important role for His187 in transition state stabilization. However, the pH studies provide no evidence for general acid catalysis, suggesting that the pK_a for His187 is outside the range studied or that this group is not in equilibrium with solvent protons. Since the NMR results presented in the following paper rule out a cationic ionization state for His187, these kinetic results are most consistent with His187 forming a *neutral* hydrogen bond with uracil O2. Further discussion of the catalytic role of His187 is presented in the following paper of this issue (*16*).

Specific Substrate Binding "Activates" Asp64 as the General Base. The data suggest that Asp64 has a relatively high pK_a in the enzyme−substrate complex, indicating a unique environment for this residue. In the free *E. coli* enzyme, Asp64 is located in a hydrophobic niche with its side chain carboxylate turned away from solvent where it forms a 2.65 Å hydrogen bond to the backbone amide proton of His134 (*14*). This indicates that it may be difficult for solvent protons to access the side chain carboxylate of Asp64 in the free enzyme. Indeed, this arrangement effectively "disarms" Asp64 from acting as a general base. However, as seen in the crystal structure of the human UDG−DNA complex, Asp64 rotates by 120° upon substrate binding, indicating that some of the substrate binding energy must be used to break the hydrogen bond to His134 (*10*). In the productive enzyme−substrate complex, the close proximity of the negatively charged phosphodiester groups of the deoxyuridine nucleotide could play a role in increasing the pK_a value for Asp64. It is attractive to suggest that some of the large specificity of UDG results from activation of Asp64 through an induced-fit mechanism involving both specific uracil flipping and conformational changes in UDG. Direct

confirmation of the catalytic role and pK_a for Asp64 awaits its assignment and titration by NMR methods.

REFERENCES

1. Friedberg, E. C. (1985) in *DNA Repair*, W. H. Freeman, New York.
2. Mosbaugh, D. W., and Bennett, S. E. (1994) *Prog. Nucleic Acid Res. Mol. Biol. 48*, 315−370.
3. Horenstein, B. A., Parkin, D. W., Estupinan, B., and Schramm, V. L. (1991) *Biochemistry 30*, 10788−10795.
4. Mentch, F., Parkin, D. W., and Schramm, V. L. (1987) *Biochemistry 26*, 921−930.
5. Zoltewicz, J. A., Clark, F. D., Sharpless, T. W., and Grahe, G. (1970) *J. Am. Chem. Soc. 92*, 1741−1750.
6. Garrett, E. R., and Mehta, P. J. (1972) *J. Am. Chem. Soc. 94*, 8542−8547.
7. Parkin, D. W., and Schramm, V. L. (1987) *Biochemistry 26*, 913−920.
8. Shapiro, R., and Kang, S. (1969) *Biochemistry 8*, 1806−1810.
9. Shapiro, R., and Danzig, M. (1972) *Biochemistry 11*, 23−29.
10. Parikh, S. S., Mol, C. D., Slupphaug, G., Bharati, S., Krokan, H. E., and Tainer, J. A. (1998) *EMBO J. 17*, 5214−5226.
11. Mol, C. D., Arvai, A. S., Slupphaug, G., Kavli, B., Alseth, I., Krokan, H. E., and Tainer, J. A. (1995) *Cell 80*, 869−878.
12. Savva, R., McAuley-Hecht, K., Brown, T., and Pearl, L. (1995) *Nature 373*, 487−493.
13. Slupphaug, G., Mol, C. D., Kavli, B., Arvai, A. S., Krokan, H. E., and Tainer, J. A. (1996) *Nature 384*, 87−92.
14. Xiao, G., Tordova, M., Jagadeesh, J., Drohat, A. C., Stivers, J. T., and Gilliland, G. L. (1999) *Proteins 35*, 13−24.
15. Stivers, J. T., Pankiewicz, K. W., and Watanabe, K. A. (1999) *Biochemistry 38*, 952−963.
16. Drohat, A. C., Xiao, G., Tordova, M., Jagadeesh, J., Pankiewicz, K. W., Watanabe, K. A., Gilliland, G. L., and Stivers, J. T. (1999) *Biochemistry 38*, 11876−11886.
17. Fasman, G. D. (1975) in *Handbook of Biochemistry and Molecular Biology: Nucleic Acids*, Vol. 1, CRC Press, Boca Raton, FL.
18. Stivers, J. T. (1998) *Nucleic Acids Res. 26*, 3837−3844.
19. Lindahl, T., Ljungquist, S., Siegert, W., Nyberg, B., and Sperens, B. (1977) *J. Biol. Chem. 252*, 3286−3294.
20. Kuzmic, P. (1996) *Anal. Biochem. 237*, 260−273.
21. Leatherbarrow, R. J. (1998) *GraFit 4.0*, Erithacus Software Ltd., Staines, U.K.
22. Varshney, U., and van de Sande, J. H. (1991) *Biochemistry 30*, 4055−4061.
23. Stivers, J. T., Abeygunawardana, C., Mildvan, A. S., Hajipour, G., and Whitman, C. P. (1996) *Biochemistry 35*, 814−823.
24. Saenger, W. (1984) in *Principles of Nucleic Acid Structure*, Springer-Verlag, New York.
25. Cleland, W. W. (1977) *Adv. Enzymol. Relat. Areas Mol. Biol. 45*, 273−387.
26. Quinn, D. M., and Sutton, L. D. (1990) in *Enzyme Mechansim from Isotope Effects* (Cook, P. F., Ed.) CRC Press, Boca Raton, FL.
27. Wells, J. A. (1990) *Biochemistry 29*, 8509−8517.
28. Sinnott, M. L. (1990) *Chem. Rev. 90*, 1171−1202.
29. Stivers, J. T., Shuman, S., and Mildvan, A. S. (1994) *Biochemistry 33*, 327−339.
30. Degano, M., Gopaul, D. N., Scapin, G., Schramm, V. L., and Sacchettini, J. C. (1996) *Biochemistry 35*, 5971−5981.
31. Guan, Y., Manuel, R. C., Arvai, A. S., Parikh, S. S., Mol, C. D., Miller, J. H., Lloyd, S., and Tainer, J. A. (1998) *Nat. Struct. Biol. 5*, 1058−1064.

BI9910878